Supplemental Material for "Critical response of a quantum van der Pol oscillator"

Shovan Dutta* and Nigel R. Cooper†
TCM Group, Cavendish Laboratory, University of Cambridge, Cambridge CB3 0HE, UK
(Dated: November 13, 2019)

CONTENTS

I. STEADY STATE OF A CLASSICAL VAN DER POL OSCILLATOR

Here we derive a closed-form expression for the steady-state response of a classical van der Pol (vdP) oscillator. As described in the main text, the equation of motion for such an oscillator is given by

$$\dot{\alpha} = \gamma_1 \alpha - \gamma_2 |\alpha|^2 \alpha + \Omega \,, \tag{S1}$$

where α is the complex amplitude, γ_1 is the negative damping, γ_2 is the nonlinear damping, and Ω is the drive. The phase of the drive is chosen such that Ω is real and positive. Hence, α is real in steady state. To solve for the response, we introduce the rescaled quantities $\tilde{\gamma}_1 \equiv \gamma_1/\gamma_2$, $\tilde{\Omega} \equiv \Omega/\gamma_2$, and $\tilde{\alpha} \equiv \alpha/\tilde{\Omega}^{1/3}$. In steady state,

$$(\tilde{\gamma}_1/\tilde{\Omega}^{2/3})\,\tilde{\alpha} - \tilde{\alpha}^3 + 1 = 0 \,. \tag{S2}$$

The only stable solution to Eq. (S2) is given by $\tilde{\alpha} = f(\tilde{\gamma}_1/\tilde{\Omega}^{2/3})$, where

$$f(x) \equiv \left(\frac{1}{2} + \sqrt{\frac{1}{4} - \frac{x^3}{27}}\right)^{1/3} + \mathrm{sgn}(x)^{2/3} \left(\frac{1}{2} - \sqrt{\frac{1}{4} - \frac{x^3}{27}}\right)^{1/3} . \tag{S3}$$

Here, sgn denotes the sign function and the powers are calculated using principal values of the arguments. Figure S1 shows the variation of $f(x)$. Note that $f(0) = 1$, i.e., $\alpha = (\Omega/\gamma_2)^{1/3}$ for $\gamma_1 = 0$. This is the characteristic nonlinear response utilized in biological sensors [S1]. Conversely, for large x, $f(x)$ can be approximated as

$$f(x) = \begin{cases} \sqrt{x} + 1/(2x) + O(x^{-5/2}) & \text{for } \; x \gg 1 \quad , \\ 1/|x| + O(x^{-4}) & \text{for } \; x \ll -1 \, . \end{cases} \tag{S4}$$

The former limit is realized for $\gamma_1 > 0$ and $\Omega/\gamma_1 \ll \sqrt{\gamma_1/\gamma_2}$, where the steady state corresponds to a perturbed limit cycle, $\alpha = \sqrt{\gamma_1/\gamma_2} + \Omega/(2\gamma_1) + O\big[(\Omega/\gamma_1)^2\sqrt{\gamma_2/\gamma_1}\big]$. The latter limit is realized for $\gamma_1 < 0$ and $\Omega/|\gamma_1| \ll \sqrt{|\gamma_1|/\gamma_2}$. Here the system is fully damped and the response grows linearly with drive, $\alpha = \Omega/|\gamma_1| + O[(\Omega/\gamma_1)^3(\gamma_2/\gamma_1)]$.

* E-mail: sd843@cam.ac.uk
† E-mail: nrc25@cam.ac.uk

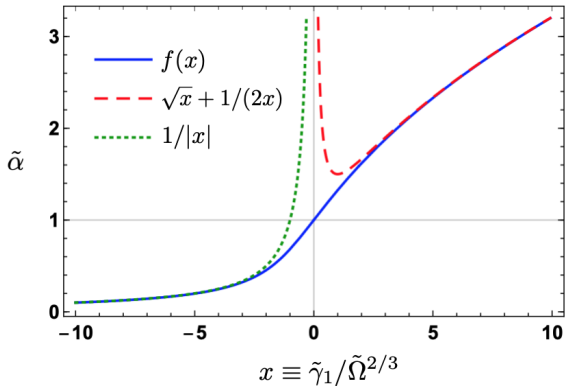

FIG. S1. Classical steady-state response as a function of rescaled parameters. The function $f(x)$ is defined in Eq. (S3).

II. RESPONSE OF A QUANTUM VAN DER POL OSCILLATOR AT WEAK DRIVES

In this section, we find analytic expressions describing the response of a weakly driven quantum vdP oscillator in special cases of interest. We start from the full dynamics in rotating frame (see main text),

$$\dot{\hat{\rho}} = [\Omega(\hat{a}^\dagger - \hat{a}), \hat{\rho}] + \gamma_1^+ \mathcal{D}[\hat{a}^\dagger]\hat{\rho} + \gamma_1^- \mathcal{D}[\hat{a}]\hat{\rho} + \gamma_2 \mathcal{D}[\hat{a}^2]\hat{\rho} \,, \tag{S5}$$

where $\hat{\rho}$ is the density matrix, $\hat{a}$ is the ladder operator, Ω is the drive amplitude, γ_1^+ is the rate of one-particle gain, γ_1^- is the rate of one-particle decay, γ_2 is the rate of two-particle decay, and $\mathcal{D}[\hat{x}]\hat{\rho} \equiv \hat{x}\hat{\rho}\hat{x}^\dagger - \{\hat{x}^\dagger\hat{x}, \hat{\rho}\}/2$. In the Fock basis $\{|n\rangle, n = 0, 1, 2, \dots\}$, Eq. (S5) can be written as

$$\begin{aligned}
\dot{\rho}_{n,n'} = {} & \Omega\left(\sqrt{n}\rho_{n-1,n'} - \sqrt{n+1}\rho_{n+1,n'} + \sqrt{n'}\rho_{n,n'-1} - \sqrt{n'+1}\rho_{n,n'+1}\right) \\
& + \gamma_1^+\left[\sqrt{nn'}\rho_{n-1,n'-1} - \left(\frac{n+n'}{2}+1\right)\rho_{n,n'}\right] \\
& + \gamma_1^-\left[\sqrt{(n+1)(n'+1)}\,\rho_{n+1,n'+1} - \frac{n+n'}{2}\rho_{n,n'}\right] \\
& + \gamma_2\left[\sqrt{(n+2)(n+1)(n'+2)(n'+1)}\,\rho_{n+2,n'+2} - \frac{n(n-1)+n'(n'-1)}{2}\rho_{n,n'}\right] .
\end{aligned} \tag{S6}$$

Note that Ω couples neighboring elements of the density matrix, whereas the dissipative terms only couple elements in the same diagonal, i.e., with $n - n' =$ constant. The response is given by $\langle\hat{a}\rangle = \mathrm{Tr}(\hat{a}\hat{\rho}) = \sum_n \sqrt{n}\rho_{n,n-1}$, where ρ is the steady-state density matrix. Since all coefficients in Eq. (S6) are real, ρ will be real and symmetric. Below we consider this steady-state response in various limits.

A. Linear response for $\gamma_1^+ = \gamma_1^- = 0$

For $\gamma_1^\pm = 0$ and weak drives $\Omega \ll \gamma_2$, any two-particle excitation decays very rapidly. Hence, the dynamics are well approximated by retaining the lowest three oscillator levels, $n = 0, 1, 2$, in Eq. (S6), which yields

$$\dot{\rho}_{00} = 2\gamma_2\rho_{22} - 2\Omega\rho_{10} \,, \tag{S7a}$$
$$\dot{\rho}_{11} = 2\Omega(\rho_{10} - \sqrt{2}\rho_{21}) \,, \tag{S7b}$$
$$\dot{\rho}_{10} = \Omega(\rho_{00} - \rho_{11}) \,, \tag{S7c}$$
$$\dot{\rho}_{21} = -\gamma_2\rho_{21} + \Omega(\sqrt{2}\rho_{11} + \rho_{20} - \sqrt{2}\rho_{22}) \,, \tag{S7d}$$
$$\dot{\rho}_{20} = -\gamma_2\rho_{20} + \Omega(\sqrt{2}\rho_{10} - \rho_{21}) \,, \tag{S7e}$$

where $\rho_{22} = 1 - \rho_{00} - \rho_{11}$. Substituting $\Omega \to 0$ into these equations, we find the undriven steady state is given by $\rho_{22} = \rho_{21} = \rho_{20} = 0$ and $\rho_{00} = \rho_{11} = 1/2$. To linear order in Ω/γ_2, Eqs. (S7b) and (S7d) yield $\rho_{10} = \sqrt{2}\rho_{21} = \Omega/\gamma_2$. Thus, the linear response is given by $\langle\hat{a}\rangle = \rho_{10} + \sqrt{2}\rho_{21} = 2\Omega/\gamma_2$, as evident in Fig. 1 of the main text.

B. Nonmonotonic response for $\gamma_1^{\pm} \ll \gamma_2$

1. $\gamma_1^+ = 0$, $0 < \gamma_1^- \ll \gamma_2$

Two-level approximation.— As the system is fully damped, we can project the dynamics at weak drives onto the manifold spanned by $n = 0$ and 1. Then Eq. (S6) reduces to

$$\dot{\rho}_{11} = 2\Omega\rho_{10} - \gamma_1^-\rho_{11} \,, \tag{S8a}$$

$$\dot{\rho}_{10} = \Omega(\rho_{00} - \rho_{11}) - (\gamma_1^-/2)\rho_{10} \,, \tag{S8b}$$

where $\rho_{00} = 1 - \rho_{11}$. In steady state, we find

$$\langle \hat{a} \rangle = \rho_{10} = \frac{2\Omega\gamma_1^-}{(\gamma_1^-)^2 + 8\Omega^2} \,. \tag{S9}$$

Thus, the response grows linearly as $\langle \hat{a} \rangle \approx 2\Omega/\gamma_1^-$ for $\Omega \lesssim \gamma_1^-$, but falls off as $\langle \hat{a} \rangle \approx \gamma_1^-/(4\Omega)$ for $\Omega \gtrsim \gamma_1^-$. This is shown by the dashed black curve in Fig. S2. We see the linear susceptibility diverges as $2/\gamma_1^-$ for $\gamma_1^- \to 0$.

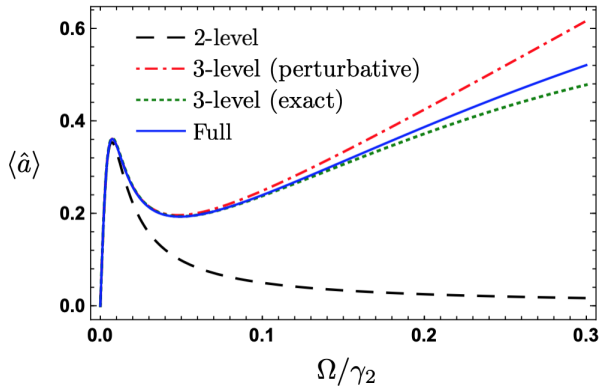

FIG. S2. Response $\langle \hat{a} \rangle$ as a function of drive Ω for $\gamma_1^+ = 0$ and $\gamma_1^-/\gamma_2 = 0.02$. The perturbative result corresponds to Eq. (S17).

Three-level approximation.— The two-level picture breaks down at large drives. As higher-energy modes come into play, the response grows again with Ω, as seen in Fig. S2. This revival can be captured by including the $n = 2$ level in the dynamics, yielding, with $\rho_{11} = 1 - \rho_{00} - \rho_{22}$,

$$\dot{\rho}_{00} = 2\gamma_2\rho_{22} - 2\Omega\rho_{10} + \gamma_1^-\rho_{11} \,, \tag{S10a}$$

$$\dot{\rho}_{10} = \Omega(\rho_{00} - \rho_{11}) + \gamma_1^-(\sqrt{2}\rho_{21} - \rho_{10}/2) \,, \tag{S10b}$$

$$\dot{\rho}_{22} = -2(\gamma_2 + \gamma_1^-)\rho_{22} + 2\sqrt{2}\Omega\rho_{21} \,, \tag{S10c}$$

$$\dot{\rho}_{21} = -(\gamma_2 + 3\gamma_1^-/2)\rho_{21} + \Omega\big[\sqrt{2}(\rho_{11} - \rho_{22}) + \rho_{20}\big] \,, \tag{S10d}$$

$$\dot{\rho}_{20} = -(\gamma_2 + \gamma_1^-)\rho_{20} + \Omega(\sqrt{2}\rho_{10} - \rho_{21}) \,. \tag{S10e}$$

Let us solve for the steady state to lowest order in γ_1^-/γ_2 and Ω/γ_2. From the last three equations, we can write

$$\rho_{22} \approx (\sqrt{2}\Omega/\gamma_2)\rho_{21} \,, \tag{S11a}$$

$$\rho_{21} \approx (\Omega/\gamma_2)\big[\sqrt{2}(\rho_{11} - \rho_{22}) + \rho_{20}\big] \,, \tag{S11b}$$

$$\rho_{20} \approx (\Omega/\gamma_2)(\sqrt{2}\rho_{10} - \rho_{21}) \,. \tag{S11c}$$

Substituting ρ_{22} and ρ_{20} into Eq. (S11b), we find

$$\rho_{21} \approx (\sqrt{2}\Omega/\gamma_2)[\rho_{11} + (\Omega/\gamma_2)\rho_{10}] \,. \tag{S12}$$

Using Eqs. (S11a) and (S12) in Eq. (S10a) yields

$$\rho_{10} \approx \left(\frac{2\Omega}{\gamma_2} + \frac{\gamma_1^-}{2\Omega}\right)\rho_{11} \,. \tag{S13}$$

Substituting this expression back into Eqs. (S12) and (S11a) yields

$$\rho_{21} \approx (\sqrt{2}\Omega/\gamma_2)\rho_{11} \,, \tag{S14}$$

$$\rho_{22} \approx 2(\Omega/\gamma_2)^2\rho_{11} \,. \tag{S15}$$

Finally, substituting Eqs. (S13)–(S15) into Eq. (S10b) and using $\rho_{00} = 1 - \rho_{11} - \rho_{22}$, we find

$$\rho_{11} \approx \frac{4\Omega^2}{(\gamma_1^-)^2 + 8\Omega^2} \,, \tag{S16}$$

which matches the two-level result. However, the response is modified as

$$\langle \hat{a} \rangle = \rho_{10} + \sqrt{2}\rho_{21} \approx \left(\frac{4\Omega}{\gamma_2} + \frac{\gamma_1^-}{2\Omega} \right) \rho_{11} \approx \frac{2\Omega}{\gamma_2} \left[\frac{\gamma_1^-\gamma_2 + 8\Omega^2}{(\gamma_1^-)^2 + 8\Omega^2} \right] , \tag{S17}$$

where we have used Eqs. (S13), (S14), and (S16). It reduces to the two-level expression in Eq. (S9) for $\Omega \ll (\gamma_1^-\gamma_2)^{1/2}$. For $\Omega \sim (\gamma_1^-\gamma_2)^{1/2} \gg \gamma_1$, we find $\langle \hat{a} \rangle \approx \gamma_1^-/(4\Omega) + 2\Omega/\gamma_2$, which attains a minimum at $\Omega = (\gamma_1^-\gamma_2)^{1/2}/(2\sqrt{2})$ and increases linearly with drive at large Ω. This nonmonotonic variation is evident in Fig. S2.

2. $0 \le \gamma_1^+, \gamma_1^- \ll \gamma_2$

In the presence of one-particle gain ($\gamma_1^+ > 0$), the undriven steady state corresponds to a dynamic equilibrium where particles flow in and out of the oscillator. When $\gamma_2 \gg \gamma_1^\pm$, the dynamics are confined to the levels $n = 0$, 1, and 2 for weak drives. We consider this three-level system, governed by the equations of motion [from Eq. (S6)]

$$\dot{\rho}_{00} = 2\gamma_2\rho_{22} - 2\Omega\rho_{10} + \gamma_1^-\rho_{11} - \gamma_1^+\rho_{00} \,, \tag{S18a}$$

$$\dot{\rho}_{10} = \Omega(\rho_{00} - \rho_{11}) + \gamma_1^-(\sqrt{2}\rho_{21} - \rho_{10}/2) - (3\gamma_1^+/2)\rho_{10} \,, \tag{S18b}$$

$$\dot{\rho}_{22} = -2(\gamma_2 + \gamma_1^-)\rho_{22} + 2\sqrt{2}\Omega\rho_{21} + 2\gamma_1^+\rho_{11} \,, \tag{S18c}$$

$$\dot{\rho}_{21} = -(\gamma_2 + 3\gamma_1^-/2)\rho_{21} + \Omega\big[\sqrt{2}(\rho_{11} - \rho_{22}) + \rho_{20}\big] + \sqrt{2}\gamma_1^+\rho_{10} \,, \tag{S18d}$$

$$\dot{\rho}_{20} = -(\gamma_2 + \gamma_1^-)\rho_{20} + \Omega(\sqrt{2}\rho_{10} - \rho_{21}) \,, \tag{S18e}$$

where $\rho_{11} = 1 - \rho_{00} - \rho_{22}$. For $\Omega = 0$, we find the steady state $\rho_{11} \approx 1 - \rho_{00} \approx \gamma_1^+/(3\gamma_1^+ + \gamma_1^-)$. Thus, negative damping leads to a finite occupation of the $n = 1$ level. For $\Omega > 0$, the steady-state analysis can be carried out following the same steps as in the last section, which yields, to lowest order in γ_1^+/γ_2, γ_1^-/γ_2, and Ω/γ_2,

$$\langle \hat{a} \rangle \approx \frac{2\Omega}{\gamma_2} \left[\frac{(\gamma_1^+ + \gamma_1^-)\gamma_2 + 8\Omega^2}{(3\gamma_1^+ + \gamma_1^-)^2 + 8\Omega^2} \right] . \tag{S19}$$

As before, we find a nonmonotonic response. For $\Omega \ll 3\gamma_1^+ + \gamma_1^-$, the response is linear, $\langle \hat{a} \rangle \approx 2\Omega(\gamma_1^+ + \gamma_1^-)/(3\gamma_1^+ + \gamma_1^-)^2$, with a slope that diverges as $\gamma_1^\pm \to 0$. For $3\gamma_1^+ + \gamma_1^- \ll \Omega \ll [(\gamma_1^+ + \gamma_1^-)\gamma_2]^{1/2}$, it falls off as $\langle \hat{a} \rangle \approx (\gamma_1^+ + \gamma_1^-)/(4\Omega)$, exhibiting negative susceptibility. For $\Omega \gg [(\gamma_1^+ + \gamma_1^-)\gamma_2]^{1/2}$, it rises again as $\langle \hat{a} \rangle \approx 2\Omega/\gamma_2$.

C. Linear response for $\gamma_1^+ = \gamma_1^- \gg \gamma_2$

Here, we derive the enhanced sensitivity for the critical condition $\gamma_1^+ = \gamma_1^- \equiv \Gamma_1 \gg \gamma_2$. We first find the undriven steady state, then consider perturbation at weak drives. At $\Omega = 0$, the steady state has no coherence. The equation of motion for the populations $p_n \equiv \rho_{n,n}$ is found by substituting $n' = n$ in Eq. (S6), which yields

$$\dot{p}_n = \Gamma_1\big[np_{n-1} + (n+1)p_{n+1} - (2n+1)p_n\big] + \gamma_2\big[(n+1)(n+2)p_{n+2} - n(n-1)p_n\big] \,. \tag{S20}$$

At $\gamma_2 = 0$, the steady state is simply given by $p_n =$ constant, i.e., the system reaches an infinite-temperature state. For $\gamma_2 > 0$, this distribution is curtailed at large n and p_n is a slowly-varying function set by the scale $\varepsilon \equiv \sqrt{\gamma_2/\Gamma_1}$. Thus, we can approximate p_n by a continuous function $p(x)$ with $x = n\varepsilon$. Then Eq. (S20) can be written as

$$xp(x-\varepsilon) + (x+\varepsilon)p(x+\varepsilon) - (2x+\varepsilon)p(x) + \varepsilon\big[(x+\varepsilon)(x+2\varepsilon)p(x+2\varepsilon) - x(x-\varepsilon)p(x)\big] = 0 \,. \tag{S21}$$

The above equation is identically satisfied up to $O(\varepsilon)$. Expanding to $O(\varepsilon^2)$, we find

$$xp''(x) + (2x^2+1)p'(x) + 4xp(x) = 0\,, \tag{S22}$$

where prime denotes $\mathrm{d}/\mathrm{d}x$. Requiring $p(x)$ to be bounded at $x=0$ leads to the unique solution $p(x) = Ce^{-x^2}$. The constant C can be determined from probability conservation $\sum_n p_n = 1$, or $(1/\varepsilon)\int_0^\infty p(x)dx = 1$, which gives

$$p(x) = (2\varepsilon/\sqrt{\pi})e^{-x^2}. \tag{S23}$$

Thus, the undriven steady state has a Gaussian number distribution of width $\sqrt{\Gamma_1/\gamma_2} \gg 1$, as shown in Fig. S3(a).

To find the linear response, we consider perturbation in the leading off-diagonal terms $\chi_n \equiv \rho_{n,n-1}$, which satisfy

$$\dot{\chi}_n = \Gamma_1\big[\sqrt{n(n-1)}\chi_{n-1} + \sqrt{n(n+1)}\chi_{n+1} - 2n\chi_n\big] + \gamma_2\big[\sqrt{n(n+2)}(n+1)\chi_{n+2} - (n-1)^2\chi_n\big] + \Omega\sqrt{n}(p_{n-1}-p_n)\,. \tag{S24}$$

This equation is simplified with the substitution $q_n \equiv \sqrt{n}\chi_n$. In steady state,

$$\Gamma_1(q_{n+1} + q_{n-1} - 2q_n) + \gamma_2\big[(n+1)q_{n+2} - (n+1/n-2)q_n\big] + \Omega(p_{n-1}-p_n) = 0\,. \tag{S25}$$

Since q_n will also be a slowly-varying function as p_n, we rewrite Eq. (S25) in terms of the continuous variable $x = n\varepsilon$,

$$q(x+\varepsilon) + q(x-\varepsilon) - 2q(x) + \varepsilon\big[(x+\varepsilon)q(x+2\varepsilon) - (x - 2\varepsilon + \varepsilon^2/x)q(x)\big] + \eta\varepsilon\big[\tilde{p}(x-\varepsilon) - \tilde{p}(x)\big] = 0\,, \tag{S26}$$

where $\eta \equiv \Omega/\Gamma_1$ and $\tilde{p}(x) \equiv p(x)/\varepsilon \sim O(1)$. Expanding Eq. (S26) to $O(\varepsilon^2)$, we find

$$q''(x) + 2xq'(x) + 3q(x) - \eta\tilde{p}'(x) = 0\,. \tag{S27}$$

Substituting $\tilde{p}'(x) = -(4/\sqrt{\pi})xe^{-x^2}$ from Eq. (S23) and using $q(x) \equiv (4\eta/\sqrt{\pi})e^{-x^2}h(x)$ yields

$$h''(x) - 2xh'(x) + h(x) + x = 0\,. \tag{S28}$$

In addition, since $q(0) = 0$, we have the boundary condition $h(0) = 0$. Then the only bounded solution to Eq. (S28) is $h(x) = x$. Therefore,

$$q(x) = (4\eta/\sqrt{\pi})xe^{-x^2}\,, \tag{S29}$$

which agrees well with numerics, as shown in Fig. S3(a). The linear response is given by

$$\langle\hat{a}\rangle = \sum_{n=0}^{\infty}\sqrt{n}\chi_n \approx \frac{1}{\varepsilon}\int_0^\infty dx\, q(x) = \frac{2\eta}{\sqrt{\pi}\varepsilon} = \frac{2\Omega}{\sqrt{\pi\Gamma_1\gamma_2}}\,. \tag{S30}$$

Hence, the linear susceptibility is $\chi \approx 2/\sqrt{\pi\Gamma_1\gamma_2}$. Figure S3(b) shows how the exact solution interpolates between this regime and that of $\Gamma_1 \ll \gamma_2$, where $\chi \approx 1/(4\Gamma_1)$ [see Sec. II B 2]. In contrast, a fully damped "passive" oscillator has a susceptibility $\chi_p = 2/\gamma_1^-$ [see Sec. II B 1]. Thus, operating the vdP oscillator in the regime $\gamma_1^+ = \gamma_1^- \gg \gamma_2$ yields a sensitivity enhancement $\chi/\chi_p \approx [\gamma_1^-/(\pi\gamma_2)]^{1/2}$.

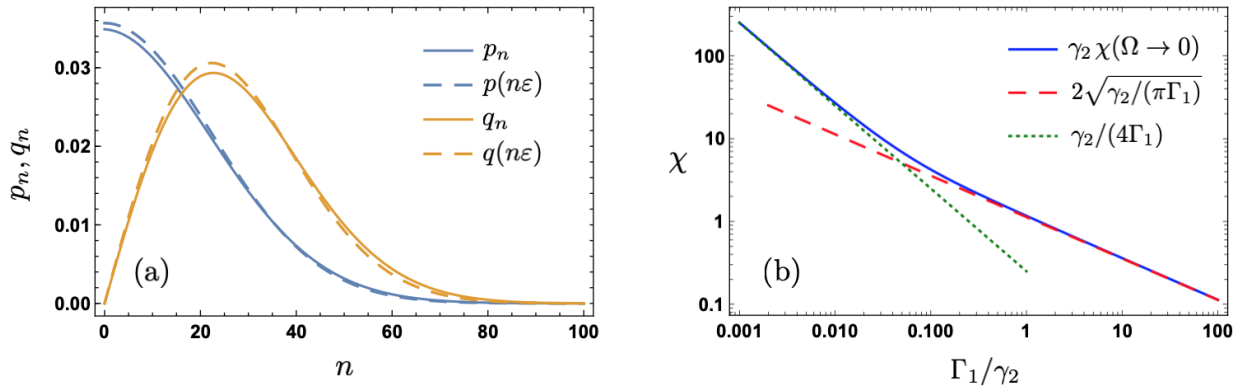

FIG. S3. (a) Steady-state occupations $p_n \equiv \rho_{n,n}$ and coherences $q_n \equiv \sqrt{n}\rho_{n,n-1}$ for $\Gamma_1/\gamma_2 = 1000$ and $\Omega \to 0$. The coherences are rescaled to show on the same axes. Solid lines are obtained from exact numerics and dashed lines correspond to Eqs. (S23) and (S29). (b) Linear susceptibility χ as a function of Γ_1/γ_2. Solid curve shows exact result and dashed curves show aymptotes.

D. Linear response for $\gamma_1^+ - \gamma_1^- \gg \gamma_2$

As we discussed in the main text, the susceptibility is enhanced much further by operating in the limit-cycle phase. Here we derive an expression for the linear response in this regime. As in the last section, we start by writing down rate equations which govern the populations of the undriven system,

$$\dot{p}_n = \gamma_1^+\big[np_{n-1} - (n+1)p_n\big] + \gamma_1^-\big[(n+1)p_{n+1} - np_n\big] + \gamma_2\big[(n+1)(n+2)p_{n+2} - n(n-1)p_n\big] \,. \tag{S31}$$

The steady state is set by the parameters $\varepsilon \equiv (\gamma_2/\gamma_1^+)^{1/2} \ll 1$ and $\zeta \equiv \gamma_1^-/\gamma_1^+ < 1$. We expect, in steady state, p_n will be peaked near the classical solution, $n^* \approx \alpha_{\rm cl}^2 = (1-\zeta)/(2\varepsilon^2)$. To find this distribution, we approximate p_n by a continuous function $p(x)$ where $x = n\varepsilon$. Then Eq. (S31) yields

$$xp(x-\varepsilon) - (x+\varepsilon)p(x) + \zeta\big[(x+\varepsilon)p(x+\varepsilon) - xp(x)\big] + \varepsilon\big[(x+\varepsilon)(x+2\varepsilon)p(x+2\varepsilon) - x(x-\varepsilon)p(x)\big] = 0 \,. \tag{S32}$$

Since $p(x)$ will be peaked near $x^* = n^*\varepsilon \sim O(1/\varepsilon)$, we shift the origin with the transformation $x = \beta/\varepsilon + y$, where $\beta \sim O(1)$. We also define $u(y) \equiv p(\beta/\varepsilon + y)$. Then expanding Eq. (S32) in powers of ε, we find

$$\varepsilon\beta(2\beta+\zeta-1)u'(y) + \varepsilon^2\big[\beta(4\beta+\zeta+1)u''(y)/2 + (4\beta+\zeta-1)\{yu'(y)+u(y)\}\big] + O(\varepsilon^3) = 0 \,. \tag{S33}$$

The linear term implies $\beta = (1-\zeta)/2$, exactly matching the classical estimate. Substituting this value for β into the quadratic term leads to the differential equation

$$(3-\zeta)u''(y) + 4yu'(y) + 4u(y) = 0 \,, \tag{S34}$$

which has a unique positive-definite solution, $u(y) = Ae^{-2y^2/(3-\zeta)}$. The integration constant A can be determined by requiring $\sum_n p_n = 1$, or $(1/\varepsilon)\int u(y)dy \approx 1$, which yields

$$u(y) \approx \varepsilon\sqrt{2/[(3-\zeta)\pi]}\, e^{-2y^2/(3-\zeta)} \,. \tag{S35}$$

From the correspondence $p_n \approx u(n\varepsilon - \beta/\varepsilon)$ and the definitions $\zeta \equiv \gamma_1^-/\gamma_1^+$, $\varepsilon \equiv (\gamma_2/\gamma_1^+)^{1/2}$, we find the undriven steady state has a Gaussian number distribution with mean $(\gamma_1^+ - \gamma_1^-)/(2\gamma_2)$ and standard deviation $[(3\gamma_1^+ - \gamma_1^-)/(4\gamma_2)]^{1/2}$. This result was also found in Ref. [S2] and agrees well with numerics, as shown in Fig. S4(a).

Next, we consider linear perturbation at weak drives. From Eq. (S6), the coherences $\chi_n \equiv \rho_{n,n-1}$ satisfy

$$\begin{aligned}\dot{\chi}_n = {}& \gamma_1^+\big[\sqrt{n(n-1)}\chi_{n-1} - (n+1/2)\chi_n\big] + \gamma_1^-\big[\sqrt{n(n+1)}\chi_{n+1} - (n-1/2)\chi_n\big] \\ & + \gamma_2\big[\sqrt{n(n+2)}(n+1)\chi_{n+2} - (n-1)^2\chi_n\big] + \Omega\sqrt{n}(p_{n-1} - p_n) \,,\end{aligned} \tag{S36}$$

where p_n are the undriven occupations. To find the steady state, we again approximate χ_n by a continuous function $v(y)$ where $\chi_n \approx v(n\varepsilon - \beta/\varepsilon)$. Following the same steps as before, we arrive at the solution

$$v(y) = 4\eta(3-\zeta)^{-3/2}\sqrt{(1-\zeta)/\pi}\, e^{-2y^2/(3-\zeta)} \,, \tag{S37}$$

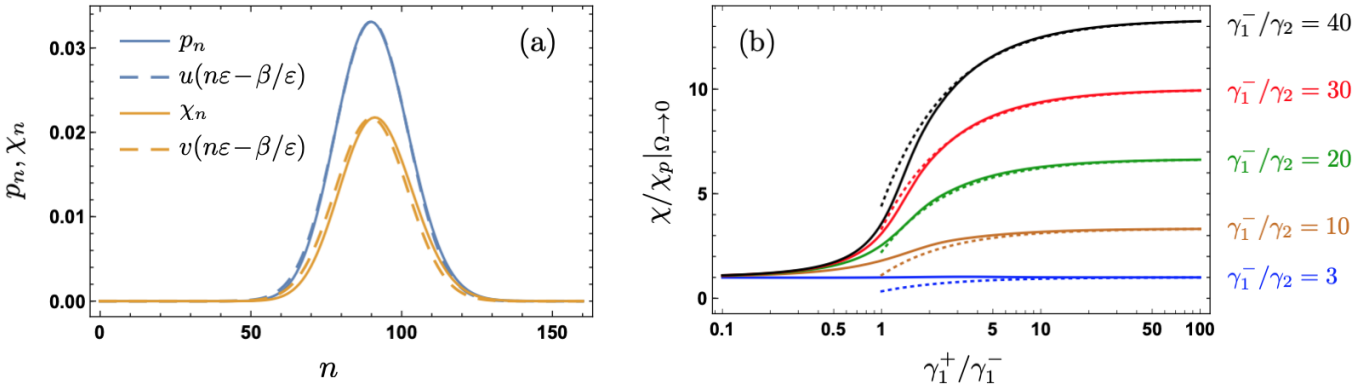

FIG. S4. (a) Steady-state populations $p_n \equiv \rho_{n,n}$ and coherences $\chi_n \equiv \rho_{n,n-1}$ for $\gamma_1^+/\gamma_2 = 200$, $\gamma_1^-/\gamma_2 = 20$, and $\Omega \to 0$. The coherences have been rescaled to show on the same axes as p_n. Solid lines correspond to exact numerics and dashed lines show perturbative results in Eqs. (S35) and (S37). (b) Linear susceptibility χ as a function of γ_1^+/γ_1^- and γ_1^-/γ_2, rescaled by the susceptibility of a passive system, $\chi_p = 2/\gamma_1^-$. Solid lines show exact results and dotted lines are obtained from Eq. (S39).

where $\eta \equiv \Omega/\gamma_1^+$. Thus, χ_n has the same Gaussian profile as p_n, as seen in Fig. S4(a). The linear response is given by

$$\langle \hat{a} \rangle = \sum_n \sqrt{n}\chi_n \approx \frac{1}{\varepsilon^2}\int_{-\beta/\varepsilon}^{\infty} \sqrt{\beta+\varepsilon y}\, v(y)dy \approx \frac{2\eta}{3\varepsilon^2}\left[1 - \frac{2\zeta}{3} + O(\zeta^2)\right] . \tag{S38}$$

Expressing η, ε, and ζ in terms of the drive and dissipation rates, we find a susceptibility

$$\chi \approx \frac{2}{3\gamma_2}\left(1 - \frac{2\gamma_1^-}{3\gamma_1^+}\right) . \tag{S39}$$

Thus, for $\gamma_1^- \ll \gamma_1^+$, χ is only limited by two-particle decay. Consequently, the sensitivity gain over a passive system, χ/χ_p, scales as γ_1^-/γ_2 [Recall: $\chi_p = 2/\gamma_1^-$]. This scaling is illustrated in Fig. S4(b).

III. MAPPING BETWEEN DENSITY MATRIX AND WIGNER FUNCTION

In this section, we review the Wigner representation of the density operator and derive an explicit mapping between the Wigner function and density matrix for an oscillator mode. The Wigner distribution was introduced in Ref. [S3] to enable the calculation of expectation values as integrals over a phase space, similar to classical ensemble averages. The Wigner function acts as a weight for such an integral representation of the density operator. For a single oscillator mode $\hat{a}$, it can be written as the expectation of a displaced parity operator [S4]

$$\hat{\Pi}(\alpha) \equiv \hat{D}(\alpha)(-1)^{\hat{a}^\dagger \hat{a}}\hat{D}^{-1}(\alpha) , \tag{S40}$$

where α is a point in phase space and $\hat{D}(\alpha) \equiv e^{\alpha\hat{a}^\dagger - \alpha^*\hat{a}}$ is a displacement operator. The Wigner function is given by

$$W(\alpha) = (2/\pi)\mathrm{Tr}\left[\hat{\rho}\hat{\Pi}(\alpha)\right] . \tag{S41}$$

Conversely, the density operator $\hat{\rho}$ can be obtained from the Wigner function as

$$\hat{\rho} = 2\int d^2\alpha\, W(\alpha)\,\hat{\Pi}(\alpha) . \tag{S42}$$

So, there is a one-to-one correspondence between $\hat{\rho}$ and W. Note the operators $\hat{\Pi}(\alpha)$ are Hermitian with eigenvalues ± 1. They can also be shown to constitute a basis for expanding any operator over the complex phase space [S5]. In particular, they satisfy the orthonormality and completeness relations

$$(4/\pi)\,\mathrm{Tr}\left[\hat{\Pi}(\alpha), \hat{\Pi}(\alpha')\right] = \delta(\alpha - \alpha')\hat{\mathbb{1}} ,$$
$$(4/\pi)\int d^2\alpha\, \langle m|\hat{\Pi}(\alpha)|m'\rangle\langle n|\hat{\Pi}(\alpha)|n'\rangle^* = \delta_{m,n}\delta_{m',n'} ,$$

where $|n\rangle$ are Fock states. Since $\hat{\Pi}(\alpha)$ are parity operators, from Eq. (S41) we see that W is real valued and uniformly bounded, $W(\alpha) \in [-2/\pi, 2/\pi]$. Further, using the property $\mathrm{Tr}[\hat{\Pi}(\alpha)] = 1/2$ in Eq. (S42), one finds

$$\int d^2\alpha\, W(\alpha) = 1 . \tag{S43}$$

Hence, $W(\alpha)$ can be interpreted as a quasiprobability distribution in phase space. In particular, one can compute the expectation of any symmetrically ordered product $\{(\hat{a}^\dagger)^n\hat{a}^m\}_S$ as an ensemble average,

$$\langle\{(\hat{a}^\dagger)^n\hat{a}^m\}_S\rangle = \int d^2\alpha\,(\alpha^*)^n\alpha^m W(\alpha) , \tag{S44}$$

which follows from using the relation $\hat{D}^{-1}(\alpha)\hat{a}\hat{D}(\alpha) = \hat{a} + \alpha\hat{\mathbb{1}}$ in Eq. (S42). The linear response $\langle\hat{a}\rangle$ corresponds to a special case of Eq. (S44) that amounts to measuring the center of mass of the Wigner distribution,

$$\langle\hat{a}\rangle = \int d^2\alpha\,\alpha\, W(\alpha) . \tag{S45}$$

In principle, Eqs. (S41) and (S42) completely specify $W(\alpha)$ in terms of $\hat{\rho}$ and *vice versa*. However, one can also find an explicit mapping between the Wigner function and the density matrix in the Fock basis. To see this, note the parity operator $(-1)^{\hat{a}^\dagger\hat{a}}$ reflects $\hat{a}$ to $-\hat{a}$, $(-1)^{\hat{a}^\dagger\hat{a}}\hat{a}(-1)^{\hat{a}^\dagger\hat{a}} = -\hat{a}$. It follows we have the identity [S4]

$$(-1)^{\hat{a}^\dagger\hat{a}}\hat{D}(\alpha)(-1)^{\hat{a}^\dagger\hat{a}} = \hat{D}(-\alpha) = \hat{D}^{-1}(\alpha)\ . \tag{S46}$$

Using the above in Eq. (S40), we can write $\hat{\Pi}(\alpha) = \hat{D}(2\alpha)(-1)^{\hat{a}^\dagger\hat{a}}$ which, when used in Eq. (S41), yields

$$W(\alpha) = (2/\pi)\sum_{n,n'}\rho_{n,n'}\langle n'|\hat{D}(2\alpha)|n\rangle(-1)^n\ . \tag{S47}$$

The matrix elements of $\hat{D}$ can be expressed in terms of associated Laguerre polynomials $L_q^{(p)}(x)$ [S5]. Thus, we find

$$W(\alpha) = (2/\pi)e^{-2|\alpha|^2}\sum_{n,n'}(-1)^n\sqrt{n!/n'!}\,(2\alpha)^{n'-n}\,L_n^{(n'-n)}(4|\alpha|^2)\,\rho_{n,n'}\ . \tag{S48}$$

The mapping can be written in a more symmetric form in polar coordinates $\alpha = re^{i\phi}$,

$$W(r,\phi) = \frac{2}{\pi}e^{-2r^2}\left[\sum_{n=0}^{\infty}(-1)^n L_n^{(0)}(4r^2)\,\rho_{n,n} + \sum_{j=1}^{\infty}(2r)^j\sum_{n=0}^{\infty}(-1)^n\frac{L_n^{(j)}(4r^2)}{\sqrt{(n+1)_j}}\left(e^{-\mathrm{i}j\phi}\rho_{n+j,n} + e^{\mathrm{i}j\phi}\rho_{n,n+j}\right)\right]\ , \tag{S49}$$

where $(x)_j$ is the Pochhammer symbol, $(x)_j = x(x+1)\ldots(x+j-1)$. We see the Wigner function has no angular variation for a purely diagonal density matrix, e.g., in the steady state of an undriven vdP oscillator. Further, elements in the j-th off diagonal contribute j units of angular momentum. Equation (S49) can be inverted using orthogonality properties of Laguerre polynomials and exponential functions to give $\rho_{n,n'}$ in terms of $W(r,\phi)$,

$$\rho_{n,n'} = (-1)^{n'}\sqrt{\frac{n'!}{n!}}\int_0^{2\pi}d\phi\,e^{\mathrm{i}(n-n')\phi}\int_0^{\infty}dr\,e^{-2r^2}(2r)^{n-n'+1}L_{n'}^{(n-n')}(4r^2)\,W(r,\phi)\ . \tag{S50}$$

IV. SIGNAL-TO-NOISE RATIO

We have focused on the response $\langle\hat{a}\rangle$ of a vdP oscillator to an external drive. An experimental measurement of this response will be subject to quantum noise. Here we estimate the signal-to-noise ratio. As we showed in Sec. III, the "signal" $\langle\hat{a}\rangle$ as well as other physical quantities can be extracted from the Wigner function $W(\alpha)$ which represents a quasiprobability distribution in phase space. From Eq. (S45), $\langle\hat{a}\rangle$ is given by the center of mass of $W(\alpha)$. The noise σ can be estimated from the spread about this center of mass,

$$\sigma^2 = \int d^2\alpha\,|\alpha - \langle\hat{a}\rangle|^2\,W(\alpha) = -|\langle\hat{a}\rangle|^2 + \int d^2\alpha\,|\alpha|^2\,W(\alpha)\ , \tag{S51}$$

where we have used Eqs. (S43) and (S45). The last integral can be evaluated from Eq. (S44), yielding

$$\sigma = \sqrt{\langle\hat{a}^\dagger\hat{a} + \hat{a}\hat{a}^\dagger\rangle/2 - |\langle\hat{a}\rangle|^2} = \sqrt{\langle\hat{n}\rangle + 1/2 - |\langle\hat{a}\rangle|^2}\ , \tag{S52}$$

where $\hat{n}$ is the number operator, $\hat{n} \equiv \hat{a}^\dagger\hat{a}$. The signal-to-noise ratio is given by $\mathrm{SNR} = \langle\hat{a}\rangle/\sigma$. We plot the response and the SNR as a function of drive and dissipation in Fig. S5, which shows one can have $\mathrm{SNR} \gtrsim 1$ while being in the quantum regime, $\langle\hat{a}\rangle \sim 1$. In Fig. S5(a), we consider the case $\gamma_1^{\pm} \ll \gamma_2$, where one finds a nonmonotonic response with increasing drive. Here $\mathrm{SNR} < 1$ as the oscillator is close to the vacuum state. Nonetheless, such states have been measured in experiments with close to 1% accuracy [S6–S12]. In Fig. S5(b), we find, for $\gamma_1^{\pm} \gg \gamma_2$, one can have both $\mathrm{SNR} > 1$ as well as a susceptibility boost over a passive oscillator, $\chi > \chi_p$.

These noise estimates also show the advantage of measuring weak signals with a quantum vdP oscillator as opposed to simply using the classical limit of the critical oscillator. Although the susceptibility can be made infinitely large in this limit, the particle-number fluctuations also diverge as $\Delta n \sim (\gamma_1^{\pm}/\gamma_2)^{1/2}$ [see Eq. (S23)]. Therefore, the SNR, in fact, vanishes for weak signals. Instead, by harnessing a quantum oscillator in the limit-cycle regime, one can enhance the "minimum detectable signal per unit time," which is an important figure-of-merit for sensors [S13].

[S1] V. M Eguíluz, M. Ospeck, Y Choe, A. J. Hudspeth, and M. O. Magnasco, "Essential Nonlinearities in Hearing," Phys. Rev. Lett. **84**, 5232 (2000).

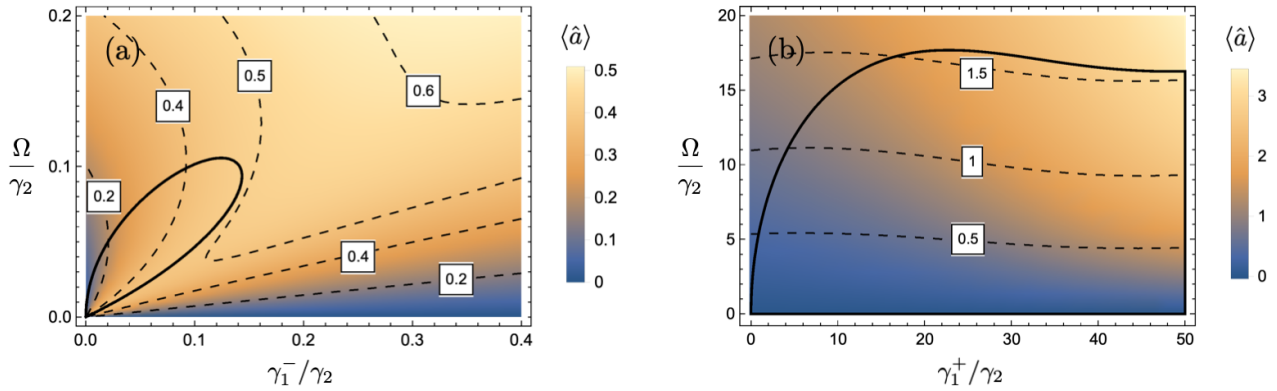

FIG. S5. Response $\langle\hat{a}\rangle$ as a function of drive Ω and dissipation rates $\gamma_1^{\pm}$. Dashed lines show contours of constant signal-to-noise ratio. (a) $\gamma_1^+ = 0$. Solid curve encloses the region over which $\mathrm{d}\langle\hat{a}\rangle/\mathrm{d}\Omega < 0$. (b) $\gamma_1^-/\gamma_2 = 30$. Below the solid curve, one finds a sensitivity enhancement over a passive system, i.e., $\mathrm{d}\langle\hat{a}\rangle/\mathrm{d}\Omega > 2/\gamma_1^-$.

[S2] V. V. Dodonov and S. S. Mizrahi, "Exact stationary photon distributions due to competition between one-and two-photon absorption and emission," J. Phys. A **30**, 5657 (1997).

[S3] E. Wigner, "On the quantum correction for thermodynamic equilibrium," Phys. Rev. **40**, 749 (1932).

[S4] K. E. Cahill and R. J. Glauber, "Density operators and quasiprobability distributions," Phys. Rev. **177**, 1882 (1969).

[S5] K. E. Cahill and R. J. Glauber, "Ordered expansions in boson amplitude operators," Phys. Rev. **177**, 1857 (1969).

[S6] K. Banaszek, C. Radzewicz, K. Wódkiewicz, and J. S. Krasiński, "Direct measurement of the Wigner function by photon counting," Phys. Rev. A **60**, 674 (1999).

[S7] A. I. Lvovsky, H. Hansen, T. Aichele, O. Benson, J. Mlynek, and S. Schiller, "Quantum state reconstruction of the single-photon Fock state," Phys. Rev. Lett. **87**, 050402 (2001).

[S8] P. Bertet, A. Auffeves, P. Maioli, S. Osnaghi, T. Meunier, M. Brune, J. M. Raimond, and S. Haroche, "Direct measurement of the Wigner function of a one-photon Fock state in a cavity," Phys. Rev. Lett. **89**, 200402 (2002).

[S9] M. Hofheinz et al., "Synthesizing arbitrary quantum states in a superconducting resonator," Nature (London) **459**, 546 (2009).

[S10] Y. Chu, P. Kharel, T. Yoon, L. Frunzio, P. T. Rakich, and R. J. Schoelkopf, "Creation and control of multi-phonon Fock states in a bulk acoustic-wave resonator," Nature (London) **563**, 666 (2018).

[S11] D. T. Smithey, M. Beck, M. G. Raymer, and A. Faridani, "Measurement of the Wigner distribution and the density matrix of a light mode using optical homodyne tomography: Application to squeezed states and the vacuum," Phys. Rev. Lett. **70**, 1244 (1993).

[S12] D. Leibfried, D. M. Meekhof, B. E. King, C. Monroe, W. M. Itano, and D. J. Wineland, "Experimental determination of the motional quantum state of a trapped atom," Phys. Rev. Lett. **77**, 4281 (1996).

[S13] C. L. Degen, F. Reinhard, and P. Cappellaro, "Quantum sensing," Rev. Mod. Phys. **89**, 035002 (2017).